Initials-Boosted Coexisting Chaos in a 2-D Sine Map and Its Hardware Implementation

Han Bao, Zhongyun Hua, *Member, IEEE*, Ning Wang, Lei Zhu, Mo Chen, and Bocheng Bao

***Abstract*—When chaotic sequences are used in engineering applications, their oscillating amplitudes need to be adjusted nondestructively. To accommodate this issue, this article presents a simple 2-D sine map. It can not only generate the chaotic sequences with high complexity, but also boost the oscillating amplitudes by switching their initial states. To show the complex dynamics of the sine map, this article investigates its control parameters-related dynamical behaviors and initials-boosted coexisting bifurcations using numerical methods. The results demonstrate that the oscillating amplitudes of chaotic sequences generated by the sine map can be nondestructively controlled by switching their initial states. This makes the sine map more suitable for many chaos-based engineering applications. Furthermore, we develop a microcontroller-hardware test platform to implement the sine map. The experimental results show that the platform synchronously outputs multichannel initials-controlled chaotic sequences. We also design a pseudorandom number generator to explore the application of the sine map.**

***Index Terms*—Chaos, chaotic sequence, hardware implementation, initial state, pseudorandom number generator, sine map.**

I. Introduction

CHAOTIC system attracts more and more attention from various academic and industrial fields due to its potential application merits [1], [2]. As a subdiscipline of nonlinear theory, chaos theory studies chaotic behaviors that are sensitive to initial conditions [3], [4]. Numerous continuous-time and discrete-time nonlinear systems can show chaotic behaviors. These systems are considered to be chaotic in the sense of mathematical definition if they are sensitive to initial conditions and topological mixing, and have dense periodic orbits. Thanks for these significant characteristics, chaotic systems were deeply studied [5] and widely applied [6], [7]. In particular, chaotic systems are usually employed in designing pseudorandom number generator (PRNG) [8], [9] or chaotic encryption algorithm-based cryptosystem [10], [11], since chaotic systems have many similar dynamical characteristics with the PRNGs and cryptosystems.

Coexisting multiple-stable states for fixed parameters, also known as "multistability", were revealed in natural, theoretical, and experimental chaotic systems [12]. Researchers found that numerous continuous-time chaotic systems can show the coexistence of multiple self-excited or hidden attractors with their isolated attraction basins [12], [13]. These systems include the nonlinear chaotic/hyperchaotic systems [14], memristor-based oscillating circuits and systems [15], memristor synapse-coupled Hopfield neural network and neuron model [16], [17], and specified offset-boostable chaotic systems [18]. Similar to the continuous-time dynamical systems, discrete-time iterative maps are also an essential category of chaotic systems and many of them can generate the coexisting multiple attractors with self-excited or hidden oscillating modes, such as the piecewise linear maps [19], multidimensional nonlinear hyperchaotic map [20], periodically modulated logistic maps [21], and multilevel dc/dc converters [22]. For a multiple-stable chaotic system, its final state depends closely on its initial conditions, which are crucial to the emergence of coexisting dynamical behaviors [14]. The initial-dependent multistability offers a great flexibility to many chaos-based engineering applications [12]. When combined with some appropriate control laws, it can be used to induce an explicit switching between different coexisting steady states [5]. Therefore, multistability control is a very important control manner in applied nonlinear science. It can lead the continuous-time or discrete-time chaotic systems to generate desired oscillating states.

The initial-dependent multistability is generally an intrinsic property of chaotic systems. The multistability can be achieved using some methods. A representative method is to import ideal memristors into existing circuits or systems [5], [15], because the memristive chaotic circuits and systems with infinite many equilibrium points are extremely easy to emerge the coexistence of initial-dependent multiple attractors. Another representative

Manuscript received January 8, 2020; revised March 4, 2020, April 1, 2020, April 23, 2020, and April 29, 2020; accepted April 30, 2020. Date of publication May 4, 2020; date of current version November 18, 2020. This work was supported in part by the National Natural Science Foundations of China under Grant 51777016, Grant 61701137, and Grant 61801054, and in part by the Natural Science Foundation of Jiangsu Province, China, under Grant BK20191451. Paper no. TII-20-0080. *(Corresponding author: Bocheng Bao.)*

Han Bao, Ning Wang, Mo Chen, and Bocheng Bao are with the School of Information Science and Engineering, Changzhou University, Changzhou 213164, China (e-mail: hi@charlesbao.com; cczuwangning@163.com; mchen@cczu.edu.cn; mervinbao@126.com).

Zhongyun Hua is with the School of Computer Science and Technology, Harbin Institute of Technology, Shenzhen 518055, China (e-mail: huazyum@gmail.com).

Lei Zhu is with the School of Electrical and Information Engineering, Jiangsu University of Technology, Changzhou 213001, China (e-mail: zhuleei@126.com).

Color versions of one or more of the figures in this article are available online at https://ieeexplore.ieee.org.

Digital Object Identifier 10.1109/TII.2020.2992438

method is to lead periodic functions to offset-boostable systems [23]. This is because these chaotic systems with periodic nonlinearities also have infinitely many equilibrium points, which permit the coexistence of offset-boosted multiple attractors herein. Recently, by combining the two representative methods above, researchers proposed a novel method by introducing the memristors with sine or cosine memductances into the offset-boostable dynamical systems [24]. This method can implement initial-boosted infinitely many coexisting bifurcations and attractors due to the emergence of initial-dependent self-similar bifurcation structures [24]. Although some effective methods were reported to implement multistability in the last few years, these methods were all applied to continuous-time chaotic systems. Thus, to achieve the coexistence of infinitely many attractors boosted by initial states in discrete-time chaotic map is attracting. However, such discrete-time chaotic maps were not reported in the previous literature.

To achieve initial-dependent multistability in discrete-time chaotic map, this article presents a novel 2-D sine map with simple algebraic structure. Analysis results show that, different from previously reported chaotic maps, the presented 2-D sine map has infinitely many line fixed points and these fixed points are unstable or critical stable, dependent on the control parameters and initial states. Such a nice property enables the 2-D sine map to exhibit control parameters-related dynamical behaviors and initials-boosted attractors' behaviors. Particularly, the 2-D sine map can provide initials-boosted infinitely many chaotic sequences, which have basically same performance indicators [24]–[27] and show better unpredictability than the chaotic sequences generated by most existing chaotic maps [28]–[32]. Therefore, the oscillating amplitudes of the chaotic sequences generated by the 2-D sine map can be nondestructively controlled by switching their initial states. This property is very important for many chaos-based engineering applications [7], and the existing chaotic maps do not have this property. Moreover, we develop a hardware test platform with synchronous multichannel outputs to implement the 2-D sine map and design a PRNG to explore its application. The test results demonstrate that the 2-D sine map can generate pseudorandom numbers (PRNs) with high randomness.

The rest of this article is organized as follows. Section II presents the 2-D sine map, and investigates its stability of the fixed points and control parameters-related dynamical behaviors. Section III studies the initials-boosted coexisting bifurcations and attractors of the 2-D sine map, and evaluates the performance of its initials-controlled chaotic sequences. Section IV implements the 2-D sine map in a microcontroller-based hardware test platform and applies it to the application of PRNG. Finally, Section V concludes this article.

II. Two-Dimensional Sine Map and Dynamical Behaviors

An effective method of producing infinitely many coexisting disconnected attractors is to introduce periodic functions into the offset-boostable dynamical systems [23]. Motivated by this strategy, this section presents a novel 2-D sine discrete-time map by introducing the sine functions into a simplest 2-D linear map. The definition of the 2-D sine map is written as

$$\begin{cases} x_{n+1} = x_n + a\sin(y_n) \\ y_{n+1} = y_n + b\sin(x_n)\sin(y_n) \end{cases} \tag{1}$$

where n is a natural number, x_n and y_n are two states at step n, and a, b are two control parameters.

A. Stability for Infinitely Many Line Fixed Points

The stability of a discrete-time map can be described using its fixed points. A fixed point of a discrete-time map is an element of its domain that maps to itself [8]. The fixed points of the 2-D sine map in (1) are denoted as $S = (x^*, y^*)$, where

$$\begin{cases} x^* = x^* + a\sin(y^*) \\ y^* = y^* + b\sin(x^*)\sin(y^*). \end{cases} \tag{2}$$

Obviously, the 2-D sine map has infinitely many line fixed points, which is expressed as

$$S = (x^*, y^*) = (\mu, m\pi) \tag{3}$$

where μ is an arbitrary constant and m is an integer number.

The fixed points of a discrete-time map can be stable or unstable. The stability of the fixed points can be reflected by the eigenvalues of its Jacobian matrix. The Jacobian matrix of the 2-D sine map at the fixed point $S = (x^*, y^*)$ is written as

$$\begin{aligned} J_S &= \begin{bmatrix} 1 & a\cos(y^*) \\ b\cos(x^*)\sin(y^*) & 1 + b\sin(x^*)\cos(y^*) \end{bmatrix} \\ &= \begin{bmatrix} 1 & \pm a \\ 0 & 1 \pm b\sin(\mu) \end{bmatrix}. \end{aligned} \tag{4}$$

The characteristic polynomial equation of (4) is derived as

$$P(\lambda) = (\lambda - 1)[\lambda - 1 \mp b\sin(\mu)]. \tag{5}$$

Let λ_1 and λ_2 be the two eigenvalues of the Jacobian matrix (4). The fixed point is stable if the absolute values of all the two eigenvalues λ_1 and λ_2 are less than 1, i.e., $|\lambda_1| < 1$ and $|\lambda_2| < 1$, and it is unstable if at least one of the absolute value of λ_1 and λ_2 is greater than 1, i.e., $|\lambda_1| > 1$ or (and) $|\lambda_2| > 1$. From (5), one can calculate the two eigenvalues as

$$\lambda_1 = 1, \lambda_2 = 1 + b\sin(\mu) \tag{6a}$$

or

$$\lambda_1 = 1, \lambda_2 = 1 - b\sin(\mu). \tag{6b}$$

Clearly, the eigenvalue λ_1 is always located on the unit circle. The eigenvalue λ_2 is always outside the unit circle when the arbitrary constant μ, i.e., initial state x_0 of the state x, satisfies that $2k\pi < \mu < (2k+1)\pi$ for $b > 0$ in (6a) or $b < 0$ in (6b) or satisfies that $(2k-1)\pi < \mu < 2k\pi$ for $b < 0$ in (6a) or $b > 0$ in (6b). This leads to that all the fixed points are unstable. On the other hand, λ_2 is always inside the unit circle when μ satisfies that $(2k-1)\pi < \mu < 2k\pi$ for $b > 0$ in (6a) or $b < 0$ in (6b) or

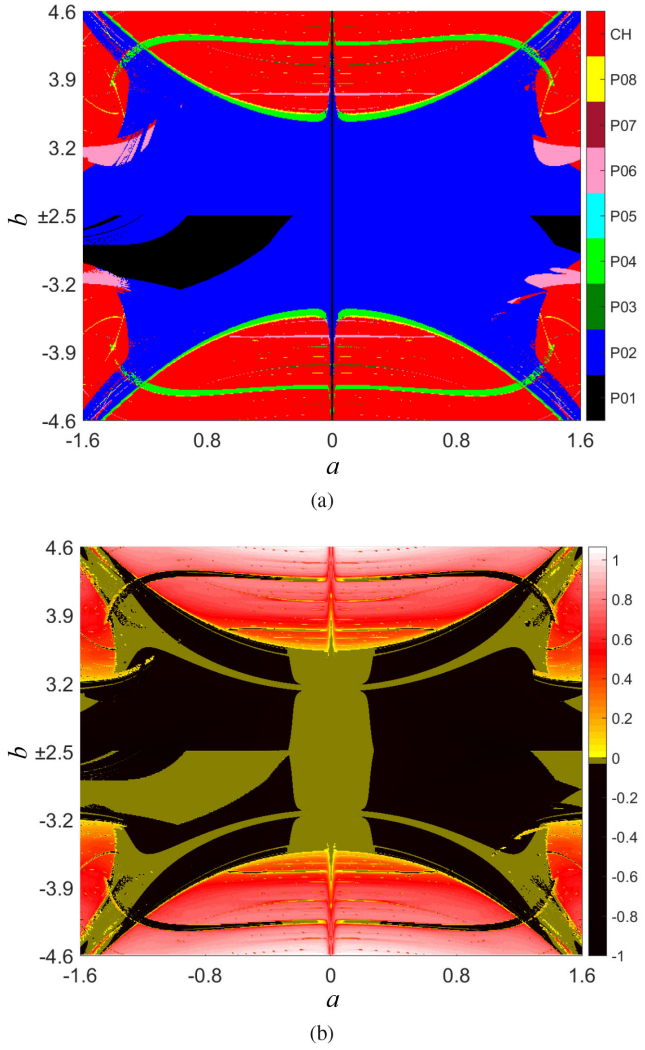

Fig. 1. 2-D dynamical behaviors distributed in the *a*-*b* parameter space under the initial states $x_0 = -2$ and $y_0 = 1$. (a) 2-D bifurcation plot by measuring the iterative sequence periodicities. (b) 2-D LLE plot by calculating the LLE.

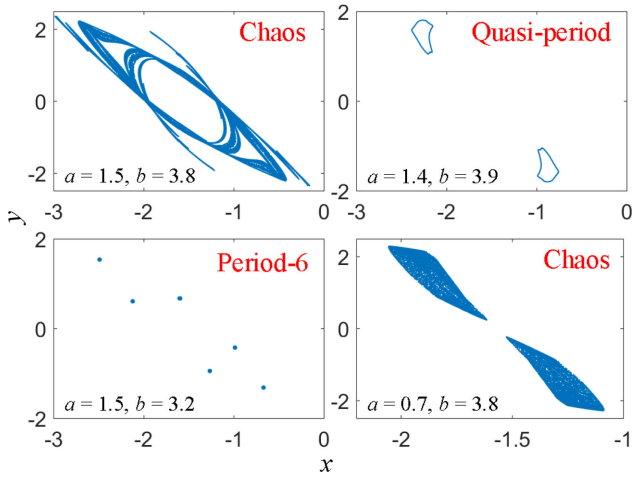

Fig. 2. Phase plane trajectories of the 2-D sine map for four sets of control parameters under the initial states $x_0 = -2$ and $y_0 = 1$. The control parameters *a*, *b* and attractor types are also provided together in the figures.

satisfies that $2k\pi < \mu < (2k+1)\pi$ for $b < 0$ in (6a) or $b > 0$ in (6b). This makes that all the fixed points are critical stable.

It is obvious that the presented 2-D sine map has infinitely many line fixed points and the stabilities of these fixed points depend on the signs of the parameter *b* and initial states. Thus, the stability of the 2-D sine is also dependent on its control parameters and initial states.

B. Control Parameters-Related Dynamical Behaviors

To analyze the properties of the 2-D sine map, we investigate its control parameters-related dynamical behaviors in aspects of 2-D bifurcation, largest Lyapunov exponent (LLE), and phase plane trajectory. The initial states of the 2-D sine map are set as fixed values, i.e., $x_0 = -2$ and $y_0 = 1$.

A colorful 2-D bifurcation plot can be depicted in the 2-D parameter space by measuring the iterative sequence periodicities of a discrete-time map [5]. Fig. 1(a) displays the 2-D bifurcation plot of the 2-D sine map with $a \in [-1.6, 1.6]$ and $b \in [-4.6, -2.5] \cup [2.5, 4.6]$. The parameter regions emerging the trajectories with different periodicities are coded using different colors. The red regions labeled by CH represent the chaos and quasi-period regions, and the other color regions labeled by P1 to P8 represent period-1 to period-8 regions, respectively. It is clearly viewed from Fig. 1(a) that the coded colors have the transitions from blue (period-2), to green (period-4), further to yellow (period-8), and finally to red (chaos), leading to the existence of period-doubling bifurcation route to chaos. In addition, a periodic window with period-4 can be clearly seen in the parameter space.

The Wolf's algorithm-based LLE is an indicator of chaos and a colorful 2-D LLE plot can be depicted in the 2-D parameter space by calculating the values of LLE of a discrete-time map. Fig. 1(b) illustrates the 2-D LLE plot of the 2-D sine map with the parameter regions used in Fig. 1(a). The parameter regions emerging the trajectories with different LLE values are coded by different colors. The yellow–red–white regions marked as the positive values represent chaos regions, the dark-yellow regions marked as the zero represent the quasi-period and period regions, and the black regions marked as the negative values represent the period regions. Therefore, the LLE plot in Fig. 1(b) is an effective way to supplement the descriptions of bifurcation plot in Fig. 1(a). As can be observed from Fig. 1(a) and (b), except for the quasi-period regions, the distributions of the period and chaos regions figured out by the 2-D bifurcation and LLE plots are consistent. Notice that the quasi-period behavior has a zero LLE but its periodicity is uncountable, similar with chaotic behavior.

Afterward, four settings of control parameter are picked from different color-coded regions given in Fig. 1. The phase plane trajectories of the 2-D sine map under these four parameter settings are obtained and shown in Fig. 2. As can be seen, four types of attractors are demonstrated, including the chaos with complex fractal structure, quasi-period with two closed curves, period-6 with six discrete points, and chaos with simple

TABLE I
LEs AND ATTRACTOR TYPES FOR DIFFERENT CONTROL PARAMETERS

a, b	LE_1, LE_2	Attractor types
1.5, 3.8	0.5390, –0. 7347	Chaotic attractor with fractal structure
1.4, 3.9	0.0007, –0. 0616	Quasi-periodic attractor with closed curves
1.5, 3.2	–0.0624, –0. 7335	Period-6 attractor with discrete points
0.7, 3.8	0.4244, –0. 1820	Chaotic attractor with two pieces

two pieces. Besides, we also calculate out the two Lyapunov exponents (LEs) of the 2-D sine map under these four parameter settings using the Wolf's algorithm. The results listed in Table I are consistent with the phase plane trajectories in Fig. 2. Consequently, the 2-D sine map has complex dynamics and its dynamical behaviors closely depend on its two control parameters.

III. INITIALS-BOOSTED BIFURCATIONS AND ATTRACTORS

This section investigates the initials-boosted bifurcations and attractors of the 2-D sine map using 1-D bifurcation and LE plots, phase plane trajectory, and local basin of attraction.

A. Initials-Boosted Coexisting Bifurcation Behaviors

To exhibit initials-boosted bifurcation behaviors of the 2-D sine map intuitively, we investigate the control parameter-related bifurcation diagrams under some specified initial states.

The control parameter a and two initial states are set as $a = 1.5, x_0 = -2 + k\pi$ ($k = 0, \pm1, \pm2, 3$), and $y_0 = 1$. The bifurcation diagrams of the state x and the LEs for $x_0 = -2$ are simulated when the control parameter b is increased in the symmetrical regions $[-4.6, -2.5]$ and $[2.5, 4.6]$, as shown in Fig. 3(a). One can see that the bifurcation diagrams for $x_0 = -2 + k\pi$ with even k have the same structure, and those for $x_0 = -2 + k\pi$ with odd k have the same structure as well. However, these two kinds of bifurcation structures have slight differences.

Next the control parameter b and two initial states are set as $b = 3.8$, $x_0 = -2$, and $y_0 = 1 + 2m\pi$ ($m = 0, \pm1, \pm2$). The bifurcation diagrams of the state y and the LEs for $y_0 = 1$ are simulated when the control parameter a is increased in the region $[-1.6, 1.6]$, as shown in Fig. 3(b). One can find that the bifurcation diagrams with the same structure are boosted by switching the initial state y_0 in a 2π cycle.

According to the results in Fig. 3(a) and (b), the coexisting bifurcations of the 2-D sine map are boosted by switching its initial states in a 2π cycle. In particular, when k and m increase to infinite, infinitely many initials-boosted bifurcations are emerged only with two dimensions. This is similar with the reported memristor initial-boosted plane bifurcations in a two-memristor-based 5-D continuous-time chaotic system [24].

B. Boosting Behaviors Induced by Two Initial States

Taking the control parameters $a = 1.5$ and $b = 3.8$ as a typical parameter setting, this subsection discloses and discusses the state boosting behaviors of the 2-D sine map by adjusting its

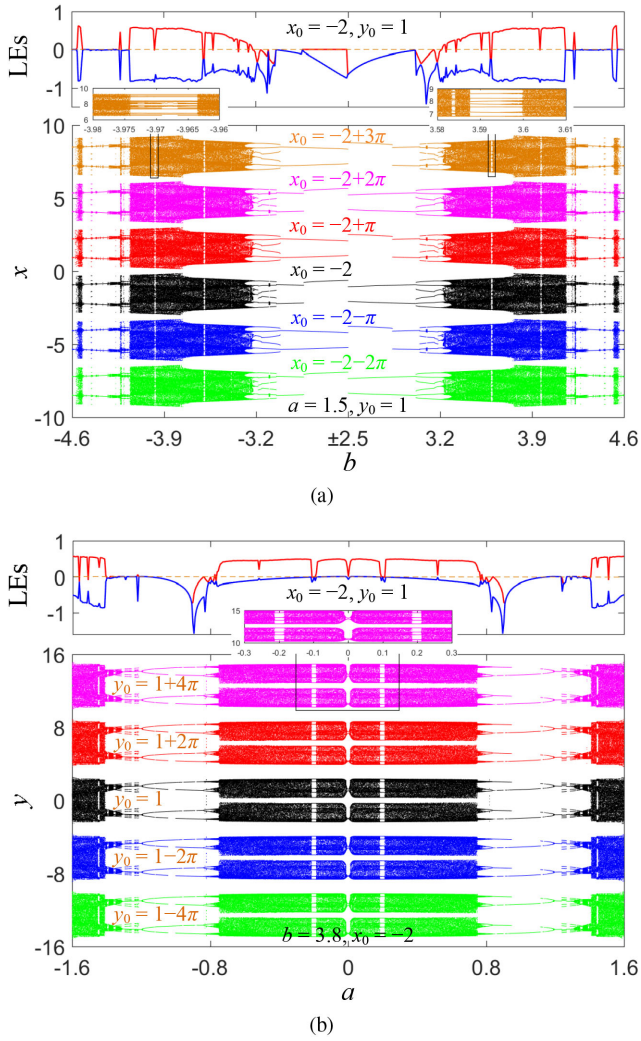

Fig. 3. Initials-boosted bifurcation behaviors along x- or y-axis. (a) For $a = 1.5$, $x_0 = -2 + k\pi$ ($k = 0, \pm1, \pm2, 3$), and $y_0 = 1$, bifurcation diagrams as b varies in $[-4.6, -2.5]$ and $[2.5, 4.6]$. (b) For $b = 3.8$, $x_0 = -2$, and $y_0 = 1 + 2m\pi$ ($m = 0, \pm1, \pm2$), bifurcation diagrams as a varies in $[-1.6, 1.6]$.

two initial states. Then, the dynamical effects of each initial state in the 2-D sine map can be readily deduced.

For fixed $y_0 = 1$, when x_0 is regarded as a boosting controller, one can plot the bifurcation diagram of the state x that is shown in Fig. 4(a). As can be seen, the linear and 1-D offset boosting is observed along the positive direction of x-axis. In this case, the chaotic attractor maintains a step change with height π in the amplitude, whereas x_0 is discretely boosted in a width 2π periodic cycle.

For fixed $x_0 = -2$, when y_0 is regarded as a boosting controller, one can also plot the bifurcation diagram of the state y that is shown in Fig. 4(b). It shows that y_0 can almost linearly boost the chaotic attractor along the positive direction of y-axis. In this case, the chaotic attractor holds a step change with height 2π in the amplitude. On the same step, y_0 has an offset of width 2π. However, there exist position mutations in three narrow regions on each step.

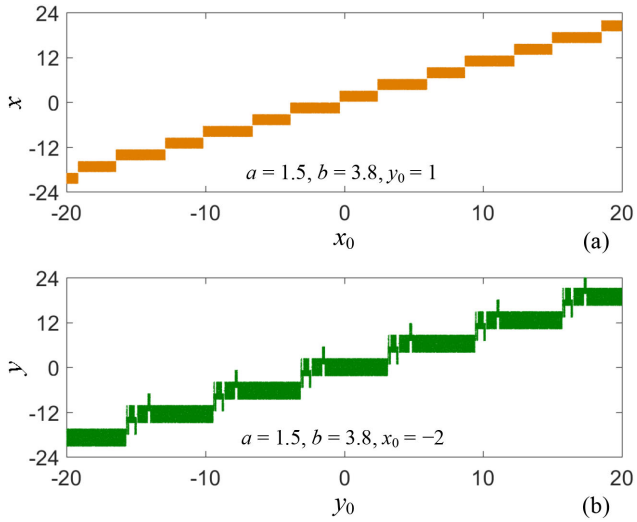

Fig. 4. For $a = 1.5$ and $b = 3.8$, bifurcation diagrams of the states x and y with respect to two initial states. (a) Initial state x_0 as a bifurcation parameter with $y_0 = 1$. (b) Initial state y_0 as a bifurcation parameter with $x_0 = -2$.

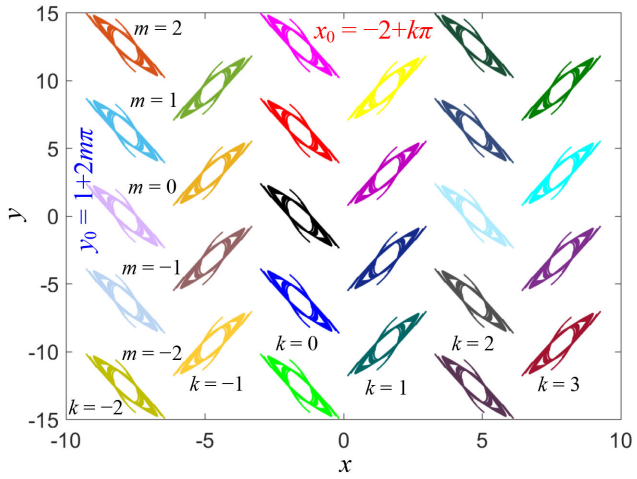

Fig. 5. Initials-boosted chaotic attractors in the xy-plane, showing the coexistence of 27 chaotic attractors with different positions, where $a = 1.5$, $b = 3.8$, $x_0 = -2 + k\pi$ ($k = 0, \pm1, \pm2, 3$), $y_0 = 1 + 2m\pi$ ($m = 0, \pm1, \pm2$). Here black for (k, m) = (0, 0), red for (k, m) = (0, 1), blue for (k, m) = (0, −1) (just a few examples).

Particularly, Fig. 4 shows that the initials-boosted dynamical behaviors of the 2-D sine map have good robustness. This property makes the presented 2-D sine map more suitable for many chaos-based engineering applications.

C. Initials-Boosted Plane Coexisting Attractors

With the phase plane trajectories in Fig. 2, we can know that the 2-D sine map for $a = 1.5$ and $b = 3.8$ displays chaos with complex fractal structure. When the initial states x_0 and y_0 are boosted, the phase plane trajectories of chaotic attractors in the xy-plane are depicted in Fig. 5, where the coexistence of 27 chaotic attractors is plotted. Note that to obtain a better visual effect, we only plot partial chaotic attractors. Much more chaotic attractors can be generated with the increase of m and k. Besides,

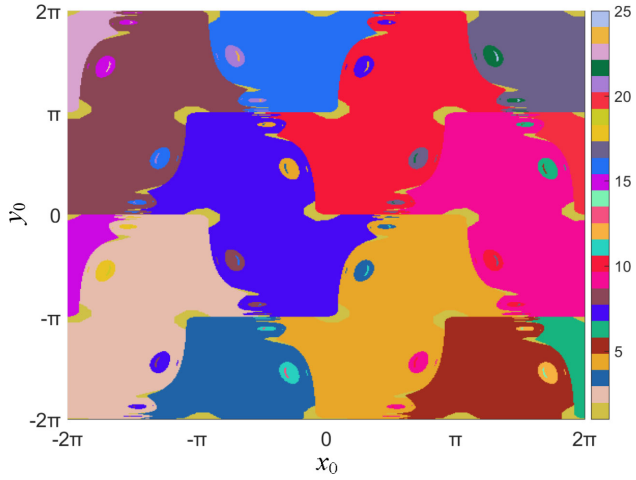

Fig. 6. For $a = 1.5$ and $b = 3.8$, chaotic basin of attraction in the $x_0 - y_0$ planes, where both x_0 and y_0 are restricted to the region $[-2\pi, 2\pi]$, and the colorbar shows the coexistence of 25 chaotic attractors with different positions.

as can be observed from Fig. 5 that the chaotic attractors for $x_0 = -2 + k\pi$ with even k have the same structure, and those for $x_0 = -2 + k\pi$ with odd k have the same structure as well. However, the extended directions of these two types of chaotic attractors are different.

The phase plane trajectories of the chaotic attractors in Fig. 5 manifest that the initials-boosted behaviors strongly depend on the two initial states. To better display these coexisting behaviors distributed on the initial plane, we plot the local basin of attraction for $a = 1.5$ and $b = 3.8$ in the $x_0 - y_0$ plane and show the results in Fig. 6. As can be seen, the regions painted by different colors stand for the attraction regions of chaotic attractors with different positions. As a result, the local basin of attraction has complex manifold topologies and basin boundaries. This involves different color blocks labeled by number 1 to 25 on the colorbar in the specific regions $[-2\pi, 2\pi] \times [-2\pi, 2\pi]$ of the initial states, indicating the coexistence of 25 chaotic attractors with different positions.

D. Performance Evaluation of Chaotic Sequences

With the initials-boosted chaotic attractors shown in Fig. 5, the initials-controlled chaotic sequences can be generated from the 2-D sine map. The control parameters are set as $a = 1.5$ and $b = 3.8$, and the initial states are assigned as $x_0 = -2 + k\pi$ ($k = 0, 1, 2$) with $y_0 = 1$ and $y_0 = 1 + 2m\pi$ ($m = -1, 0, 1$) with $x_0 = -2$, respectively. Thus, six chaotic sequences can be generated by the 2-D sine map and they are shown in Fig. 7. Actually, there are five different chaotic sequences and two chaotic sequences are repetitive. These numerical results indicate that the oscillating amplitudes of the generated chaotic sequences can be controlled by switching the initial states.

The dynamical performances of the initials-controlled chaotic sequences generated by the 2-D sine map can be evaluated using the Wolf's algorithm-based LEs (LE_1, LE_2), Kaplan–Yorke dimension (D_{KY}) [25], permutation entropy (PE) [26], correlation dimension (CorDim) [27], and spectral entropy (SE)

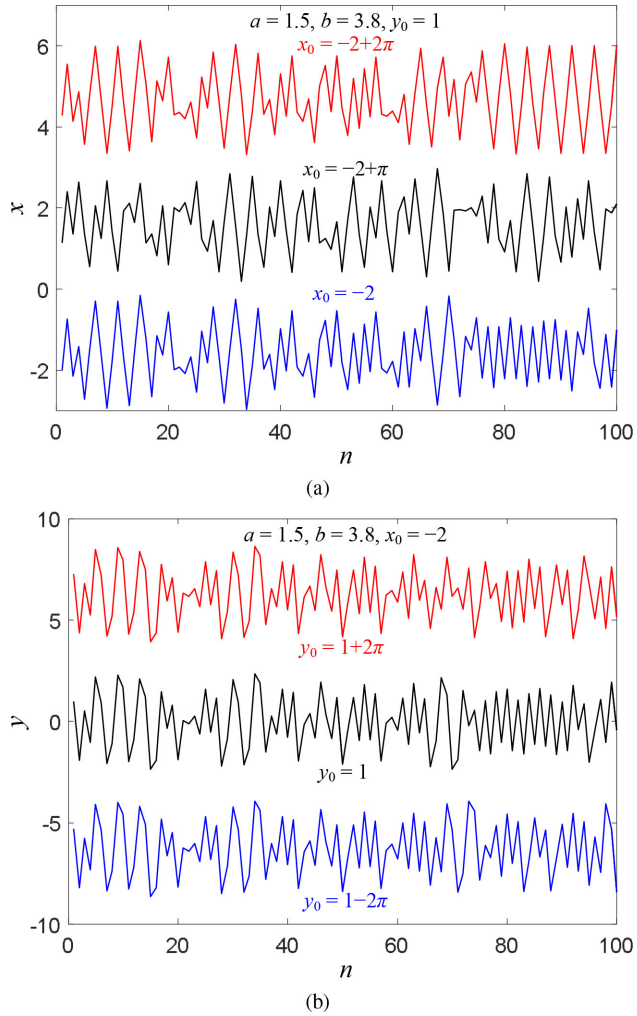

Fig. 7. Initials-controlled chaotic sequences of 2-D sine map, demonstrating the emergence of initials-controlled robust chaos. (a) Initial state x_0-boosted chaotic sequences along the x-axis. (b) Initial state y_0-boosted chaotic sequences along the y-axis.

TABLE II
PERFORMANCE EVALUATIONS FOR CHAOTIC SEQUENCES OF 2-D SINE MAP

x_0, y_0	LE_1, LE_2	D_{KY}	PE	CorDim	SE
$-2+2\pi$, 1	0.5377, –0. 7338	1.7325	4.6579	1.3416	0.9237
$-2+\pi$, 1	0.5295, –0. 7393	1.7166	4.6672	1.3450	0.9207
-2, 1	0.5390, –0. 7347	1.7336	4.6675	1.3321	0.9235
-2, $1+2\pi$	0.5318, –0. 7262	1.7321	4.6628	1.3496	0.9223
-2, $1-2\pi$	0.5393, –0. 7215	1.7474	4.6666	1.3586	0.9242

[24]. Note that the length of all chaotic sequences is set to 10^5. The calculated results for the five different chaotic sequences plotted in Fig. 7 are listed in Table II. As can be seen, these initials-controlled chaotic sequences have almost the same results for different indictors. The slight differences are caused by the numerical calculation errors. This indicates that the chaotic sequences of the 2-D sine map have high controllability by the initial states and that the initials-controlled chaos is robust.

TABLE III
PERFORMANCE COMPARISONS FOR CHAOTIC SEQUENCES OF SOME 2-D MAPS

Chaotic maps	Parameters	Initial states	LLE	CorDim	SE
This Sine map	(1.5, 3.8)	(−2, 1)	0.5390	1.3321	0.9235
Hénon map [28]	(1.4, 0.3)	(0, 0)	0.4202	1.2255	0.9107
Map CF_a [29]	(1.2, 2)	(0.27, 0.28)	0.1364	1.1768	0.4512
Map NFI_a [30]	–	(0.93, −0.44)	0.0640	1.0293	0.3076
Map NEM_1 [31]	2	(1.7, −0.39)	0.1170	1.3322	0.5361
2D-SLM map [32]	(1, 3)	(0.1, 0.1)	0.4648	1.1096	0.9376
E-Hénon map [8]	(1, 2)	(0, 0.1)	1.0816	1.6675	0.9502

Table III compares the dynamical performance of the presented 2-D sine map with those of six reported 2-D chaotic maps within their respective chaotic regions. These reported 2-D chaotic maps include the Hénon map [28], chaotic map with closed curve fixed points (Map CF_a) [29], hidden chaotic map (Map NFI_a) [30], first quadratic chaotic map (Map NEM_1) [31], sine Logistic modulation (2D-SLM) map [32], and enhanced Hénon (E-Hénon) map [8]. Generally, a 2-D discrete-time map has two LEs and its LLE determines the chaotic dynamics of this map. One can see that the presented 2-D sine map possesses considerably larger LLE than most existing 2-D chaotic maps except for the E-Hénon map. Meanwhile, the 2-D sine chaotic map can achieve larger CorDim and SE than many existing 2-D chaotic maps. The comparative results indicate that the initials-controlled chaotic sequences generated by the presented 2-D sine map have better unpredictability. Usually, the chaotic sequences of high-dimensional discrete-time chaotic maps [8] may have more outstanding dynamical performance. However, these chaotic maps do not have the striking nondestructive control property by switching the initials states.

IV. HARDWARE TEST PLATFORM AND APPLICATION

This section implements the 2-D sine map in a hardware test platform and applies it to the application of PRNG.

A. Microcontroller-Based Hardware Implementation

Due to the properties of ultralow power, and strong controllability, the pony-size and low-cost microcontroller is widely used in industrial electronics [9]. Hence, we develop a microcontroller-based hardware test platform to implement the presented 2-D sine map. The hardware devices contain one microcontroller MSP430F149 (16-bit), two D/A converters TLV5638 (12-bit), and other needful peripheral circuits. The microcontroller is utilized for implementing the 2-D sine map, the two D/A converters provide multichannel analog voltage output, and the digital oscilloscope directly displays the results.

First, program the 2-D sine map using C language according to its mathematical expression, and then download the program to the microcontroller. The control parameters of the 2-D sine map are set as $a = 1.5$ and $b = 3.8$, and its initial states are assigned as $x_0 = -2 + k\pi$ ($k = 0, 1, 2$) and $y_0 = 1 + 2m\pi$

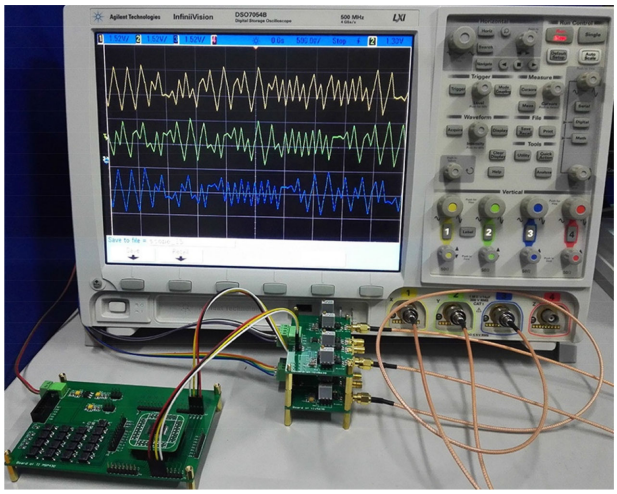

Fig. 8. Hardware devices of the microcontroller-based test platform and the generated chaotic sequences.

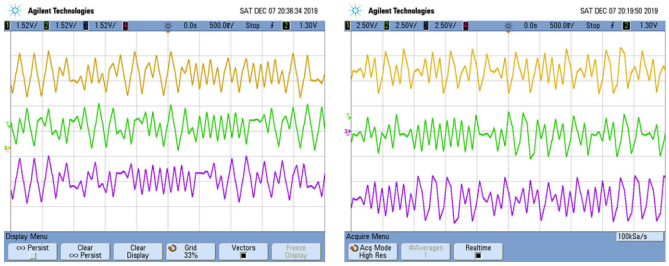

(a) (b)

Fig. 9. Initials-controlled chaotic sequences measured from the hardware test platform. (a) Initial state x_0-boosted chaotic sequences along the x-axis. (b) Initial state y_0-boosted chaotic sequences along the y-axis.

$(m = -1, 0, 1)$. After the control parameters and initial states are preloaded in the hardware platform, run the program in the microcontroller and three-channel chaotic sequences of the 2-D sine map can be synchronously generated.

Fig. 8 displays the snapshot of the hardware experimental prototype. The generated three-channel chaotic signals are captured by the digital oscilloscope and shown in Fig. 9. It shows that two sets of three-channel chaotic sequences along x- and y-axis randomly oscillate in the separately fixed amplitude ranges. The test results demonstrate the correctness and feasibility of the hardware implementation of the 2-D sine map, and also indicate the generation of initial-controlled robust chaos in the hardware devices.

B. Application in Pseudorandom Random Number Generator

Chaotic systems are widely studied in generating PRNs and chaos-based PRNGs have attracted increasing attention in industrial applications [1], [2]. When a chaotic system is used to generate PRNs, its dynamical performance highly determines the performance of the generated PRNs. Because the presented 2-D sine map has complex dynamics, it can show high performance in the application of PRNG [7]–[9].

Here, a PRNG is designed using the initials-controlled chaotic sequences generated by the 2-D sine map. Suppose $X = \{x_1, x_2, \ldots, x_n\}$ or $X = \{y_1, y_2, \ldots, y_n\}$ is a generated chaotic sequence by the 2-D sine map, a set of PRNs P_i with amplitude $[0, N)$ can be obtained as follows:

$$P_i = \lfloor (X_i + |X_{\min}|) \cdot K \rfloor \bmod N \tag{7}$$

where K is a positive integer, $X_{\min}$ is the minimum value of X, and $\lfloor \cdot \rfloor$ denotes the least integer not larger than "·" Afterward, the corresponding pseudorandom binary streams are obtained by converting the integer PRNs into the binary streams.

A PRGN with high performance is expected to generate PRNs with high randomness. Here, we use the National Institute of Standards and Technology (NIST) SP800-22 test suit [33] to test the performance of the pseudorandom bitstreams generated by the proposed PRGN. The NIST SP800-22 is a convinced random number test suite that includes 15 subtests. Each subtest is designed to find out the nonrandom area within a binary stream. The significance level α is used to measure the statistical error and it is suggested as 0.01. The length of binary stream should be no smaller than 10^6. To obtain statistically meaningful results and reasonably accurate confidence interval, we here set the number of binary stream sample as 1000.

When generating PRNs using the PRNG in (7), our experiment sets N as 256 and choose the parameter K as a large positive integer, i.e., $K = 10^6$. Since each integer PRN P_i is with amplitude $[0, N)$, it can be converted into an 8-bit binary stream. Thus, a binary stream of length 10^6 can be obtained using a chaotic sequence of length 125 000. Two collections of binary streams are generated from the chaotic sequences as follows. First, set the control parameters of the 2-D sine map as $a = 1.5$ and $b = 3.8$, and set its initial states as $x_0 = -2 + \pi + \epsilon$ and $y_0 = 1$, where ϵ is a tiny value that are randomly generated within interval $(0, 0.001)$. When ϵ is randomly configured 1000 times, 1000 chaotic sequences with the state x can be generated. Then, a collection of 1000 binary streams of length 10^6 can be obtained from the chaotic sequences. Similarly, when setting its initial states as $x_0 = -2$ and $y_0 = 1 + 2\pi + \epsilon$, and keeping the control parameters unchanged, another collection of 1000 binary streams of length 10^6 can be obtained using the state y.

The two collections of binary streams are tested using the NIST SP800-22 test suite and Table IV summarizes the testing results. According to the calculation in [33], the minimum pass proportions are approximately 0.980 for a sample size 1000. The $P\text{-}value_T$ is to measure the uniform distribution of the P-*values* and is calculated as

$$P\text{-value}_T = \text{igamc}(9/2, \chi^2/2) \tag{8}$$

where igamc$(\cdot)$ is the incomplete gamma function and

$$\chi^2 = \sum_{i=1}^{10} \frac{(F_i - s/10)^2}{s/10} \tag{9}$$

where uniformly divide the data range into ten subintervals and F_i is the number of P-*value* in the ith subinterval. If the obtained

TABLE IV
NIST STATISTICAL TEST RESULTS OF THE PROPOSED PRNG

No.	Test index	PRNG generated by x		PRNG generated by y	
		Prop.	$P\text{-value}_T$	Prop.	$P\text{-value}_T$
01	Frequency	0.989	0.657933	0.987	0.011144
02	Block Frequency	0.992	0.952152	0.991	0.028625
03	Cum. Sums (F)	0.990	0.502247	0.988	0.201189
	Cum. Sums (R)	0.988	0.890582	0.988	0.807412
04	Runs	0.985	0.560545	0.986	0.942198
05	Longest Runs	0.987	0.514124	0.986	0.763677
06	Rank	0.994	0.801865	0.995	0.034942
07	FFT	0.987	0.707513	0.982	0.227180
08	NOT*	0.982	0.373625	0.981	0.103753
09	OT	0.992	0.239266	0.991	0.635037
10	Universal	0.993	0.209948	0.985	0.271619
11	Approx. Entropy	0.992	0.114040	0.987	0.383827
12	Random Exc.*	0.9818	0.908091	0.9834	0.867692
13	Random Exc. Var.*	0.9818	0.908091	0.9868	0.278001
14	Serial (1st sub-test)	0.994	0.316052	0.986	0.858002
	Serial (2nd sub-test)	0.989	0.109435	0.985	0.867692
15	Linear complexity	0.992	0.540204	0.991	0.735908

*Nonoverlapping template test, Random excursions test, and Random excursions variant test are comprised of 148, 8, and 18 subtests, respectively. The worst result of multiple subtests is reported.

$P\text{-value}_T$ is larger than or equal to 0.0001, the *P-value*s are considered to uniformly distribute to pass the related subtest. As can be seen from the table, when using the two collections of 1000 binary streams as the test input, respectively, all the generated pass proportions are larger than the minimum pass proportions, and all the $P\text{-value}_T$s are larger than 0.0001. This indicates that the presented 2-D sine map can generate a large number of PRNs owning high randomness.

V. CONCLUSION

The chaotic dynamics of nonlinear systems was generally dependent on their control parameters. This made the generated chaotic sequences difficult to guarantee consistent dynamics with the evolution of their control parameters. To address this issue, this article presented a 2-D sine map. The chaotic attractors of chaotic sequences generated by the 2-D sine map were repeatedly boosted in the phase space by switching its initial states. This can ensure that the boosted chaotic sequences were robust to chaos and thereby the oscillating amplitudes can be nondestructively controlled. These advantages allowed the presented 2-D sine map to have the potential application merits.

Due to the infinitely many line fixed points, the 2-D sine map displayed complex dynamics under different control parameters and initial states. The control parameters-related dynamical behaviors and initials-boosted attractors' behaviors were explored using multiple numerical methods. Performance evaluations clarify that the initials-boosted chaotic sequences have almost the same indicators and they have better unpredictability than those chaotic sequences generated by many existing chaotic maps. To show the implementation, a microcontroller-based hardware test platform was developed, which can synchronously output the initials-boosted chaotic sequences. To demonstrate its applications, the 2-D sine map was applied to design PRNG. Performance analysis showed that the 2-D sine map can generate random numbers with high randomness, which is suitable for chaos-based engineering applications. Certainly, implementing the 2-D sine map-based PRNG and cryptosystem for secure communications [34] and image encryptions [35] deserves further study.

ACKNOWLEDGMENT

The authors would like to thank the anonymous reviewers for their valuable comments and suggestions that greatly contribute to improving the quality of the manuscript.

REFERENCES

[1] X. Meng, P. Rozycki, J.-F. Qiao, and B. M. Wilamowski, "Nonlinear system modeling using RBF networks for industrial application," *IEEE Trans. Ind. Informat.*, vol. 14, no. 3, pp. 931–940, Mar. 2018.
[2] Y. Deng, H. Hu, W. Xiong, N. N. Xiong, and L. Liu, "Analysis and design of digital chaotic systems with desirable performance via feedback control," *IEEE Trans. Syst., Man, Cybern., Syst.*, vol. 45, no. 8, pp. 1187–1200, Aug. 2015.
[3] C. Li, B. Feng, S. Li, J. Kurths, and G. Chen, "Dynamic analysis of digital chaotic maps via state-mapping networks," *IEEE Trans. Circuits Syst. I*, vol. 66, no. 6, pp. 2322–2335, Jun. 2019.
[4] S. H. Luo and Y. D. Song, "Chaos analysis-based adaptive backstepping control of the microelectromechanical resonators with constrained output and uncertain time delay," *IEEE Trans. Ind. Electron.*, vol. 63, no. 10, pp. 6217–6225, Oct. 2016.
[5] M. Chen, M. Sun, H. Bao, Y. Hu, and B. Bao, "Flux-charge analysis of two-memristor-based Chua's circuit: Dimensionality decreasing model for detecting extreme multistability," *IEEE Trans. Ind. Electron.*, vol. 67, no. 3, pp. 2197–2206, Mar. 2020.
[6] D. Abbasinezhad-Mood and M. Nikooghadam, "Efficient anonymous password-authenticated key exchange protocol to read isolated smart meters by utilization of extended Chebyshev chaotic maps," *IEEE Trans. Ind. Informat.*, vol. 14, no. 11, pp. 4815–4828, Nov. 2018.
[7] Z. Hua, B. Zhou, and Y. Zhou, "Sine chaotification model for enhancing chaos and its hardware implementation," *IEEE Trans. Ind. Electron.*, vol. 66, no. 2, pp. 1273–1284, Feb. 2019.
[8] Z. Hua, Y. Zhou, and B. Bao, "Two-dimensional sine chaotification system with hardware implementation," *IEEE Trans. Ind. Informat.*, vol. 16, no. 2, pp. 887–897, Feb. 2020.
[9] M. Bakiri, C. Guyeux, J.-F. Couchot, L. Marangio, and S. Galatolo, "A hardware and secure pseudorandom generator for constrained devices," *IEEE Trans. Ind. Informat.*, vol. 14, no. 8, pp. 3754–3765, Aug. 2018.
[10] Y. Zhang and X. Wang, "A new image encryption algorithm based on non-adjacent coupled map lattices," *Appl. Soft Comput.*, vol. 26, pp. 10–20, Jan. 2015.
[11] Y. Zhang and X. Wang, "A symmetric image encryption algorithm based on mixed linear–nonlinear coupled map lattice," *Inf. Sci.*, vol. 273, pp. 329–351, Jul. 2014.
[12] A. N. Pisarchik and U. Feudel, "Control of multistability," *Phys. Rep.*, vol. 540, no. 4, pp. 167–218, Jul. 2014.
[13] D. Dudkowski, S. Jafari, T. Kapitaniak, N. V. Kuznetsov, G. A. Leonov, and A. Prasad, "Hidden attractors in dynamical systems," *Phys. Rep.*, vol. 637, no. 3, pp. 1–50, Jun. 2016.
[14] J. Ma, F. Wu, G. Ren, and J. Tang, "A class of initials-dependent dynamical systems," *Appl. Math. Comput.*, vol. 298, 65–76, Apr. 2017.
[15] F. Corinto and M. Forti, "Memristor circuits: Bifurcations without parameters," *IEEE Trans. Circuits Syst. I, Reg. Papers*, vol. 64, no. 6, pp. 1540–1551, Jun. 2017.
[16] C. Chen, J. Chen, H. Bao, M. Chen, and B. Bao, "Coexisting multi-stable patterns in memristor synapse-coupled Hopfield neural network with two neurons," *Nonlinear Dyn.*, vol. 95, no. 4, pp. 3385–3399, Mar. 2019.
[17] H. Bao, A. Hu, W. Liu, and B. Bao, "Hidden bursting firings and bifurcation mechanisms in memristive neuron model with threshold electromagnetic induction," *IEEE Trans. Neural Netw. Learn. Syst.*, vol. 31, no. 2, pp. 502–511, Feb. 2020.

[18] Q. Lai, C. Chen, X. Zhao, J. Kengne, and C. Volos, "Constructing chaotic system with multiple coexisting attractors," *IEEE Access*, vol. 7, pp. 24051–24056, 2019.
[19] M. Patra, "Multiple attractor bifurcation in three-dimensional piecewise linear maps," *Int. J. Bifurc. Chaos*, vol. 28, no. 10, 2018, Art. no. 1830032.
[20] H. Natiq, S. Banerjee, M. R. K. Ariffin, and M. R. M. Said, "Can hyperchaotic maps with high complexity produce multistability?" *Chaos*, vol. 29, Jan. 2019, Art. no. 011103.
[21] T. U. Singh, A. Nandi, and R. Ramaswamy, "Coexisting attractors in periodically modulated logistic maps," *Phys. Rev. E*, vol. 77, no. 6, Jun. 2008, Art. no. 066217.
[22] Z. T. Zhusubaliyev, E. Mosekilde, and E. V. Pavlova, "Multistability and torus reconstruction in a DC–DC converter with multilevel control," *IEEE Trans. Ind. Informat.*, vol. 9, no. 4, pp. 1937–1946, Nov. 2013.
[23] C. Li and J. C. Sprott, "An infinite 3-D quasiperiodic lattice of chaotic attractors," *Phys. Lett. A*, vol. 382, no. 8, pp. 581–587, Feb. 2018.
[24] H. Bao, M. Chen, H. Wu, and B. Bao, "Memristor initial-boosted coexisting plane bifurcations and its extreme multi-stability reconstitution in two-memristor-based dynamical system," *Sci. China Technol. Sci.*, vol. 63, no. 4, pp. 603–613, Apr. 2020.
[25] P. Frederickson, J. L. Kaplan, E. D. Yorke, and J. A. Yorke, "The Liapunov dimension of strange attractors," *J. Differential Equ.*, vol. 49, no. 2, pp. 185–207, Aug. 1983.
[26] C. Bandt and B. Pompe, "Permutation entropy: A natural complexity measure for time series," *Phys. Rev. Lett.*, vol. 88, no. 17, Apr. 2002, Art. no. 174102.
[27] J. Theiler, "Efficient algorithm for estimating the correlation dimension from a set of discrete points," *Phys. Rev. A*, vol. 36, no. 9, pp. 4456–4462. Nov. 1987.
[28] M. Hénon, "A two-dimensional mapping with a strange attractor," *Commun. Math. Phys.*, vol. 50, no. 1, pp. 69–77, Feb. 1976.
[29] H. Jiang, Y. Liu, Z. Wei, and L. Zhang, "A new class of two-dimensional chaotic maps with closed curve fixed points," *Int. J. Bifurcation Chaos*, vol. 29, no. 7, 2019, Art. no. 1950094.
[30] H. Jiang, Y. Liu, Z. Wei, and L. Zhang, "Hidden chaotic attractors in a class of two-dimensional maps," *Nonlinear Dyn.*, vol. 85, no. 4, pp. 2719–2727, Sep. 2016.
[31] S. Panahi, J. Sprott, and S. Jafari, "Two simplest quadratic chaotic maps without equilibrium," *Int. J. Bifurcation Chaos*, vol. 28, no. 12, 2018, Art. no. 1850144.
[32] Z. Hua, Y. Zhou, C. M. Pun, and C. L. P. Chen, "2D sine logistic modulation map for image encryption," *Inf. Sci.*, vol. 297, pp. 80–94, Mar. 2015.
[33] A. L. Rukhin *et al.*, *A statistical Test Suite for Random and Pseudorandom Number Generators for Cryptographic Applications*. National Institute of Standards and Technology Gaithersburg, MD, USA, Apr. 2010.
[34] C. Li, Y. Zhang, and E. Y. Xie, "When an attacker meets a cipher-image in 2018: A year in review," *J. Inf. Secur. Appl.*, vol. 48, Oct. 2019, Art. no. 102361.
[35] X. Wang, L. Teng, and X. Qin, "A novel colour image encryption algorithm based on chaos," *Signal Process.*, vol. 92, no. 4, pp. 1101–1108, Apr. 2012.

Han Bao received the B.S. degree in landscape design from Finance and Economics University of Jiangxi, Jiangxi, China, in 2015 and the M.S. degree in art and design from Changzhou University, Changzhou, China, in 2018. He is currently working toward the Ph.D. degree in nonlinear system analysis and measurement technology at Nanjing University of Aeronautics and Astronautics, Nanjing, China.

He visited the Computer Science Department, University of Auckland, New Zealand, in 2019. His current research interest includes memristive neuromorphic circuit, nonlinear circuits and systems, and artificial intelligence.

Zhongyun Hua (Member, IEEE) received the B.S. degree from Chongqing University, Chongqing, China, in 2011, and the M.S. and Ph.D. degrees from University of Macau, Macau, China, in 2013 and 2016, respectively, all in software engineering.

He is currently an Associate Professor with the School of Computer Science and Technology, Harbin Institute of Technology, Shenzhen, China. His current research interests include chaotic system, chaos-based applications, and multimedia security.

Ning Wang received the B.S. and M.S. degree in electronic information engineering and computer application technology from Changzhou University, Changzhou, China, in 2015 and 2018, respectively. He is currently working toward the Ph.D. degree in control science and engineering at Tianjin University, China.

His current research interests include nonlinear circuits and systems, chaotic circuits and systems, and nonlinear system control. He is author and coauthor of 15 peer reviewed articles in these areas.

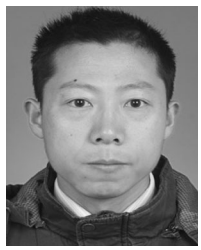

Lei Zhu received the B.S. degree in mechanical engineering from Yangzhou University, Yangzhou, China, in 2002, and the M.S. degree in optical engineering from Yanshan University, Qinhuangdao, China, in 2006.

He is currently an Associate Professor with the School of Electrical and Information Engineering, Jiangsu University of Technology, Changzhou, China. His current research interest mainly focuses on nonlinear circuits and systems.

Mo Chen received the B.S. degree in information engineering, and the M.S. and the Ph.D. degrees in electromagnetic field and microwave technology from Southeast University, Nanjing, China, in 2003, 2006, and 2009, respectively.

Between 2009 and 2013, she was a Lecturer with Southeast University, Nanjing, China. She is currently an Associate Professor with the School of Information Science and Engineering, Changzhou University, Changzhou, China. Her current research interest includes memristor and its application circuits, and other nonlinear circuits and systems.

Bocheng Bao received the B.S. and M.S. degrees in electronic engineering from the University of Electronics Science and Technology of China, Chengdu, China, in 1986 and 1989, respectively, and the Ph.D. degree in information and communication engineering, Nanjing University of Science and Technology, Nanjing, China, in 2010.

He has more than 20 years experience in the industry and was with several enterprises as a Senior Engineer and the General Manager. From 2008 to 2011, he was a Professor with the School of Electrical and Information Engineering, Jiangsu University of Technology, Changzhou, China. Then, he was a Full Professor with the School of Information Science and Engineering, Changzhou University, Changzhou, China. In 2013, he visited the Department of Electrical and Computer Engineering, University of Calgary, Calgary, AB, Canada. His current research interests include bifurcation and chaos, analysis and simulation in neuromorphic circuits, power electronic circuits, and nonlinear circuits and systems. Prof. Bao was the recipient of The IET Premium Awards in 2018.